Journal of Medicinal Chemistry

Article

Double-winged 3-Hydroxypyrimidine-2,4-diones: Potent and Selective Inhibition against HIV-1 RNase H with Significant Antiviral Activity

Sanjeev Kumar V Vernekar, Jing Tang, Bulan Wu, Andrew D. Huber, Mary C Casey, Nataliya S. Myshakina, Daniel J. Wilson, Jayakanth Kankanala, Karen A. Kirby, Michael A Parniak, Stefan G. Sarafianos, and Zhengqiang Wang

J. Med. Chem., **Just Accepted Manuscript** • Publication Date (Web): 19 May 2017

ACS Publications

Journal of Medicinal Chemistry is published by the American Chemical Society. 1155 Sixteenth Street N.W., Washington, DC 20036

Double-winged 3-Hydroxypyrimidine-2,4-diones: Potent and Selective Inhibition against HIV-1 RNase H with Significant Antiviral Activity

Sanjeev Kumar V. Vernekar [a], Jing Tang [a], Bulan Wu[#] [a], Andrew D. Huber [b], Mary C. Casey [c], Nataliya Myshakina [d], Daniel Wilson [a], Jayakanth Kankanala [a], Karen A. Kirby [c], Michael A. Parniak [e], Stefan G. Sarafianos [c, f] and Zhengqiang Wang [a]*

[a] *Center for Drug Design, Academic Health Center, University of Minnesota, Minneapolis, MN 55455, USA*

[b] *Department of Veterinary Pathobiology, Christopher S. Bond Life Sciences Center, University of Missouri, Columbia, MO 65211, USA*

[c] *Department of Molecular Microbiology and Immunology, Christopher S. Bond Life Sciences Center, University of Missouri School of Medicine, Columbia, MO 65211, USA*

[d] *Department of Natural Science, Chatham University, 1 Woodland Road, Pittsburgh, PA, 15232, USA*

[e] *Department of Microbiology & Molecular Genetics, University of Pittsburgh School of Medicine, Pittsburgh, PA 15219, USA*

[f] *Department of Biochemistry, University of Missouri, Columbia, MO 65211, USA*

Abstract

Human immunodeficiency virus (HIV) reverse transcriptase (RT)-associated ribonuclease H (RNase H) remains the only virally encoded enzymatic function yet to be exploited as an antiviral target. One of the possible challenges may be that targeting HIV RNase H is confronted with a steep substrate barrier. We have previously reported a 3-hydroxypyrimidine-2,4-dione (HPD) subtype that potently and selectively inhibited RNase H without inhibiting HIV in cell

culture. We report herein a critical redesign of the HPD chemotype featuring an additional wing at the C5 position that led to drastically improved RNase H inhibition and significant antiviral activity. Structure-activity-relationship (SAR) concerning primarily the length and flexibility of the two wings revealed important structural features that dictate the potency and selectivity of RNase H inhibition as well as the observed antiviral activity. Our current medicinal chemistry data also revealed a correlation between RNase H biochemical inhibition and the antiviral activity.

Introduction

Current management of HIV infection relies primarily on highly active antiretroviral therapy (HAART)[1], a combination therapy typically consisting of three antivirals with at least two distinct mechanisms of action. HAART has proved largely effective with numerous FDA-approved drugs, particularly those targeting the three virally encoded enzymes: RT, integrase (IN) and protease (PR).[2] However, since current antiviral therapy does not cure HIV infection,[3-4] the required long duration of HAART is expected to eventually lead to the selection of resistant viral strains and treatment failure. Novel antivirals with unique resistance profiles, particularly those against viral functions not yet targeted by current HAART, are crucial to combating drug-resistant viruses. One such novel target is RT-associated RNase H activity.[5-6] RT encodes two distinct domains and enzymatic functions (Figure 1a): a polymerase (pol) domain which carries out both RNA-dependent and DNA-dependent viral DNA polymerization; and an RNase H domain which degrades the RNA strand from the RNA/DNA heteroduplex intermediate and processes primers for the synthesis of both the minus strand and plus strand viral DNA. Numerous nucleoside RT inhibitors (NRTIs)[6-8] and non-nucleoside RT inhibitors (NNRTIs)[6, 8-9] targeting the pol domain have been approved by FDA. However, inhibitors of RT-associated

RNase H have yet to enter the development pipeline, as bona fide RNase H inhibitors remain elusive. It is noteworthy that while many compounds were reported to inhibit RNase H in biochemical assays, none conferred antiviral activity *via* RNase H inhibition. Nevertheless, attenuated RNase H activities through active site mutation correlated well with reduced levels of HIV replication in cell culture,[10] indicating that the functions of RNase H are required for HIV replication and that small molecules effectively inhibiting RNase H functions in a similar manner should confer antiviral activities.

(A)

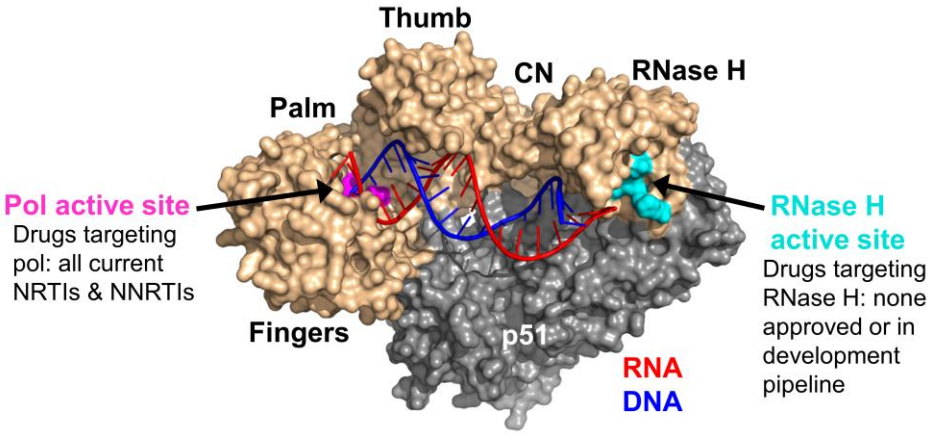

(B)

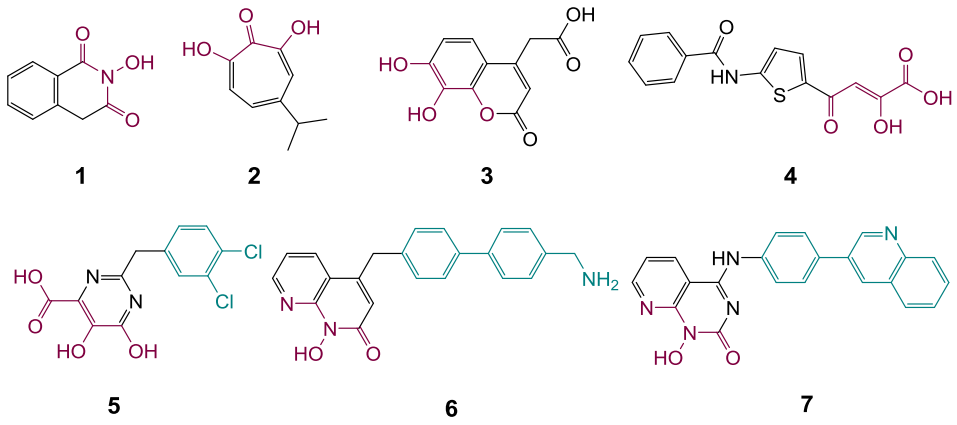

Figure 1. Targeting HIV RT. (A) Structure of RT (created with PyMOL based on PDB code 4PQU[11]). The active site of pol is shown in pink and that of RNase H in cyan. The RNA (red) / DNA (blue) heteroduplex engages with both active sites. Pol is targeted by all current NRTIs and NNRTIs while bona fide inhibitors of RNase H remain unknown. CN = connection subdomain. (B) Major chemotypes reported as HIV RNase H active site inhibitors. All chemotypes contain a chelating triad (magenta); scaffolds **5**–**7** also feature an aryl or biaryl moiety (cyan) connected through a methylene or amino linker.

Current design of RNase H inhibitors exploits mainly the active site, which closely resembles that of HIV IN,[12] and the dependence of catalysis on two divalent metal ions. Accordingly, reported RNase H inhibitors typically entail a pharmacophore core similar to integrase strand transfer inhibitors (INSTIs) featuring a chelating triad (Figure 1b).[13] Chemotypes known for active site RNase H inhibition include 2-hydroxyisoquinolinedione (HID, **1**),[14-16] β-thujaplicinol (**2**),[17] dihydroxycoumarin (**3**),[18] diketoacid (**4**),[19] pyrimidinol carboxylic acid (**5**),[20] hydroxynaphthyridine (**6**)[21] and pyridopyrimidone **7**.[22] Such a strategy has proved viable in achieving potent RNase H inhibition in biochemical assays. A remaining challenge, however, is that the observed biochemical inhibition has not been translated into significant antiviral phenotype in cell culture. While other factors may contribute to the hurdle in achieving antiviral activity with RNase H-targeting small molecules, the tight binding of much larger DNA/RNA substrates to RNase H active site may pose a biochemical barrier too steep for the competing small molecules to overcome. We have long been interested in developing potent and selective RNase H inhibitors.[23-28] Particularly interesting is our reported[25] HPD[29-30] subtype **8** designed to specifically inhibit RNase H. Potent and selective RNase H inhibition was indeed achieved with many analogues; however, none showed significant antiviral activity.[25] Interestingly, when **8** is

docked into the RNase H active site, two distinct binding modes are observed (Figure 2A) with or without nucleic acid substrate. Without the substrate, **8** binds in a way that the chelating core (the body) directly interacts with two divalent metal ions while the C-6 biarylamino moiety (the wing) makes a key contact with H539 (Figure 2A, left). However, in the presence of the competing nucleic acid substrate, the wing of **8** is forced to flip, resulting in a possible loss of the key interaction with H539 (Figure 2A, right). This suggests that **8** may not be able to effectively compete against the substrate to confer antiviral activity. The two docking poses depicted in Figure 2A allowed us to envision a double-winged subtype (**9**) that could make optimized interactions with H539 with or without substrate. This was confirmed *via* docking of **9** in the presence of the substrate (Figure 2B), wherein one of the two wings does interact with both the H539 and the substrate. However, the synthesis of subtype **9** turned out to be challenging. Redesign of the C-5 wing by replacing the amino linkage with a synthetically more accessible carboxamide linkage[23] generated subtype **10** (Figure 2B). These unsymmetrically double-winged HPD analogues demonstrated highly potent and selective inhibition against RNase H and inhibited HIV-1 in cell culture. Herein we report the chemical synthesis, biochemical evaluation against RNase H, pol and INST, and antiviral activities against HIV-1 of the new HPD subtype **10**.

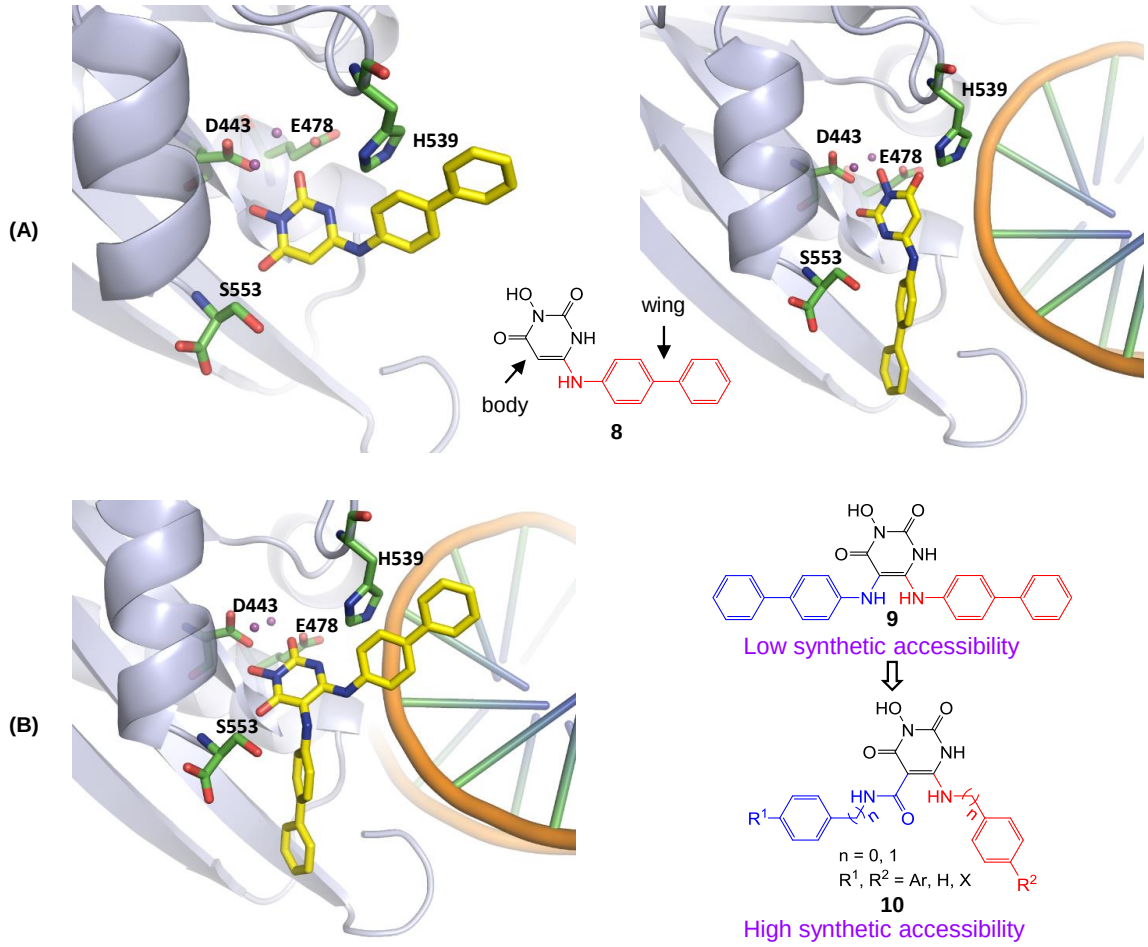

Figure 2. Design of double-winged HPD subtype **10**. (A) Docking of single-winged subtype **8** into RNase H active site with (right) or without (left) substrate. With the substrate binding to the active site, the wing of **8** is forced to flip and the key interaction with H539 is lost. (B) Introducing a second wing (in blue) at the C-5 position of HPD allows interactions with H539 and nucleic acid substrate (left, docking of **9**). Unsymmetrically double-winged subtype **10** is designed due to synthetic accessibility.

Results and Discussion

Chemistry. Analogues of subtype **10** were synthesized based on our previously reported procedures (Schemes 1–2).[23] The commercially available hydroxyurea **11** was first protected

with a benzyl group, and the resulting 1-(benzyloxy)urea **12** was subjected to condensation with diethyl malonate under microwave irradiation to yield cyclic compound **13**. Treatment of **13** with $POCl_3$ in the presence of $BnEt_3NCl$ produced the key chloride intermediate **14** in good yield. The preparation of **14** allowed the sequential assembling of the two wings: first the C-6 wing was introduced by reacting the chloride with amines in the presence of *N*,*N*-dimethylaniline under microwave irradiation to give C-6 amino products **15** in moderate to good yields; then the C-5 wing was assembled *via* a carboxamidation with commercially available or *in situ* generated isocyanates to furnish double-winged compounds **16** in good yields. Alternatively, the C-5 carboxamidation can be achieved *via* a two-step procedure (Scheme 2) to avoid use of the unpleasant nitrobenzene as the solvent. In this case, the C-5 site of **15** was first carboxylated with phenyl chloroformate to give phenylesters **17** which were subsequently aminated with amines under conventional heating to deliver **16** (Scheme 2). Finally, the synthesis of the desired compounds **10** was completed through debenzylation *via* TFA-mediated hydrolysis or catalytic hydrogenation.

Scheme 1[a] Synthesis of subtype **10**

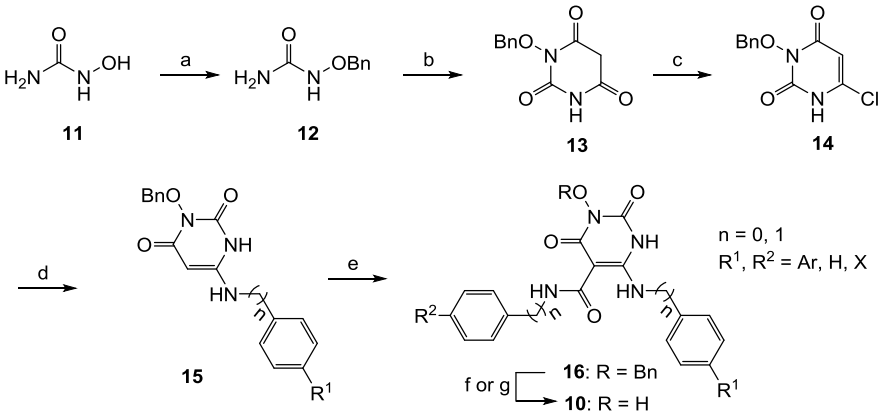

[a] Reagents and conditions: a) KOH, BnBr, MeOH, reflux, 6 h, 91%; b) $CH_2(COOEt)_2$, NaOEt, microwave, 150 ºC, 20 min, 58%; c) $POCl_3$, $BnEt_3NCl$, 50 ºC, 6 h, 88%; d) R^1-NH_2, *N*,*N*-dimethylaniline, microwave, 170 ºC, 20–25 min, 49-81%; e) R^2NCO (or R^2CON_3), $PhNO_2$, microwave, 210 ºC, 20–40 min, 52–96%; f) Pd/C, H_2, 40~50 Psi, MeOH, 4–6 h, 76–92%; g) TFA, microwave, 120 ºC, 35–55 min, 19–84%.

Scheme 2[a] Alternative synthesis of chemotype **10**

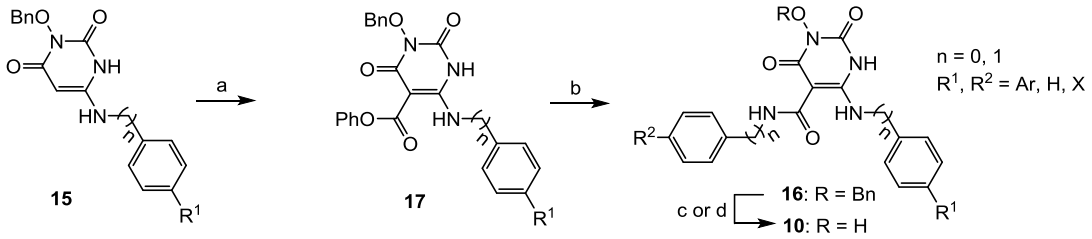

[a]Reagents and conditions: a) $ClCO_2Ph$, pyridine, 60 ºC, 2h, 61–63%; b) amines, dioxane, 120 ºC, 8–12 h, 58–67%; c) Pd/C, H_2, 40~50 Psi, MeOH, 4–6 h, 76–92%; d) TFA, microwave, 120 ºC, 35–55 min, 19–84%.

The design of chemotype **10** analogues concerned mainly the variation of the two wings, specifically their length (short aryl *vs.* long biaryl) and the flexibility (flexible when n=1 *vs.* non-flexible when n=0). The effects of substituents at the end of each wing were also considered. A total of 30 analogues were designed and synthesized.

Biology. All analogues of chemotype **10** were first evaluated biochemically for inhibition against HIV RT-associated RNase H. Due to the tight binding by the substrate to RNase H active site, achieving ultra-potent RNase H inhibition would be essential for inhibitors to effectively compete against the substrate. Importantly, RNA cleavage by RNase H is required at multiple stages of reverse transcription and could involve at least three distinct modes[31]: the random

internal cleavages, the DNA 3′ end directed and polymerase dependent cleavages and the RNA 5′ end directed cleavages. Our biochemical assay used the HTS-1 DNA / RNA substrate specifically designed to probe random internal cleavages, the dominant mode of RNA cutting. In addition, selective inhibition of the RNase H function of RT is often accompanied by the inhibition of RT pol. The functions of RT entail a delicate spatial and temporal relationship between the RNase H and pol domains, and implications of inhibiting one domain on the functions of the other are complicated.[5] Moreover, active site inhibitors of RNase H also tend to inhibit INST due to similar active site fold and mechanism of catalysis.[12] To gauge the selectivity in RNase H inhibition by our double-winged compounds, assays measuring the activity of RT pol and INST were included in our biochemical studies. Finally, selected analogues were also tested for cytotoxicity and antiviral potency in a MAGI assay.[32] Previously reported HIV RNase H inhibitor trihydroxybenzoyl naphthyl hydrazone (THBNH)[33] was used as the control in all RT assays and two FDA-approved INSTIs, raltegravir (RAL)[34] and dolutegravir (DTG)[35], were used as controls in both the INST assay and the MAGI antiviral assay. All biological results are summarized in Tables 1-2. Since the design of chemotype **10** was based on the single-winged HPD scaffold, compound **8** is listed for comparison.

Biochemical Inhibition. The first set of compounds (**10a-c**) features a long and nonflexible C5 wing (the left wing) while maintaining the same C-6 wing (the right wing) as in reference compound **8**. Biochemical testing showed that the addition of the new C-5 wing decreased the RNase H inhibitory potency by 4-5 fold while slightly increasing the potency against RT pol (**10a-c** vs **8**, Table 1), two undesired trends. The same C-6 wing is preserved with the second set of compounds (**10d-j**); however, replacing the long and nonflexible C-5 wing with a short and flexible wing resulted in drastically improved potencies against RNase H (40–110 nM) along

with significantly decreased RT pol inhibition (**10d**, **10f**, **10i** and **10j**, Table 1). These observations support a desired potent and selective RT RNase H inhibitory profile and indicate that a short C-5 wing should be preferred over a long one. The next set of compounds (**10k-n**, Table 1) features a long C-6 wing with a flexible methylene group. Significantly, all four analogues exhibited strong biochemical potency against RNase H without inhibiting RT pol at concentrations up to 10 μM. The benefit of the added flexibility in the C-6 wing is evident *via* direct comparison of two pairs of analogues: **10k** (RNase H IC_{50} = 0.14 μM; pol IC_{50} > 10 μM) *vs.* **10a** (RNase H IC_{50} = 1.0 μM; pol IC_{50} = 1.8 μM) and **10n** (RNase H IC_{50} = 0.054 μM; pol IC_{50} > 10 μM) *vs.* **10d** (RNase H IC_{50} = 0.11 μM; pol IC_{50} >10 μM). From this set of compounds, two additional structure-activity-relationship (SAR) trends concerning the C-5 wing were revealed: 1) adding a flexible methylene group to the C-5 wing did not produce discernable inhibitory benefit (**10l** *vs.* **10k**; **10n** *vs.* **10m**); 2) a short wing (**10m-n**) produced better RNase H inhibition than a long wing (**10k-l**), which corroborates the observation from the first two sets of compounds. Accordingly, our further SAR efforts focused on analogues with a short C-6 wing (**10o-t**). When directly compared with corresponding analogues containing a long C-6 wing (**10p** *vs.* **10l**; **10q** *vs.* **10m; 10r** *vs.* **10n**), the short wing appeared to confer about two-fold higher potencies. Clearly, both C-5 and C-6 positions prefer a short wing for optimized RNase H inhibition and the combination of two short wings produced exceptionally potent RNase H inhibition (**10q-t**, IC_{50} = 0.016–0.056 μM) and significantly less inhibition against RT pol ($IC_{50} \geq$ 10 μM).

Table 1. Biochemical studies of chemotype **10** against RT HIV RNase H and Pol, and INST.

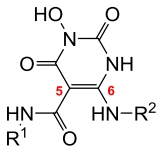

10a-dd

Compound	*R^1*	*R^2*	*RT RNase H IC_{50} [a] (μM)*	*RT pol IC_{50} [a] (μM)*	*INST IC_{50}[a] (μM)*
8	--	--	0.25	2.0	NT [b]
10a	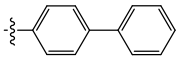	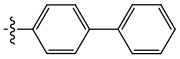	1.0 ± 0.3	1.8 ± 0.5	*>100*
10b	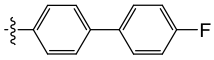	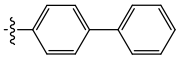	0.97 ± 0.3	1.6 ± 0.5	>100
10c	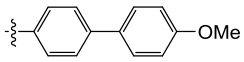	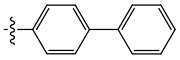	1.2 ± 0.3	1.4 ± 0.2	>100
10d	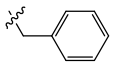	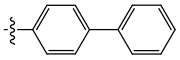	0.11 ± 0.06	>10	23 ± 9
10e	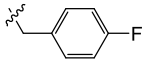	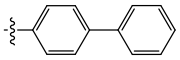	0.047 ± 0.03	>10	>100
10f	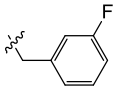	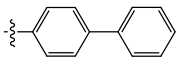	0.049 ± 0.02	>10	>100
10g	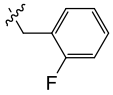	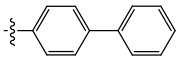	0.040 ± 0.01	>10	>100
10h	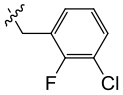	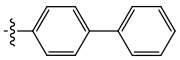	0.059 ± 0.03	>10	>100
10i	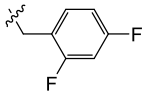	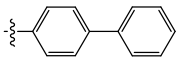	0.077 ± 0.03	8.6 ± 5.7	>100
10j	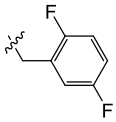	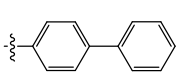	0.050 ± 0.04	9.5 ± 0.5	>100

10k	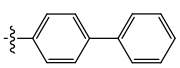	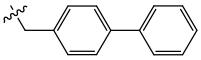	0.14 ± 0.09	>10	>100
10l	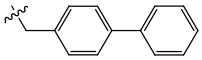	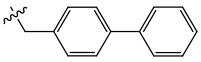	0.11 ± 0.06	>10	>100
10m		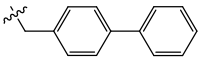	0.047 ± 0.02	>10	>100
10n	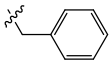	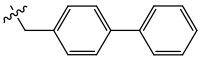	0.054 ± 0.02	>10	1.6 ± 0.7
10o	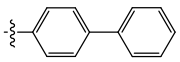	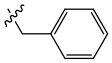	0.12 ± 0.09	>10	>100
10p	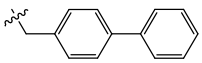	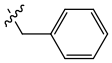	0.038 ± 0.003	>10	>100
10q		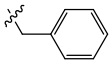	0.027 ± 0.002	>10	>100
10r	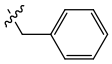	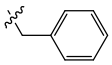	0.032 ± 0.006	>10	0.14 ± 0.03
10s	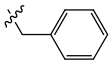		0.056 ± 0.02	>10	0.23 ± 0.04
10t			0.016 ± 0.003	>10	1.5 ± 0.2
10u	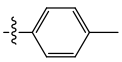	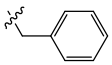	0.019 ± 0.005	~10	34 ± 8
10v	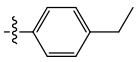	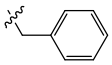	0.054 ± 0.04	~10	>100
10w	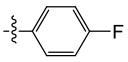	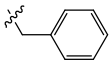	0.019 ± 0.003	~10	71 ± 33

10x	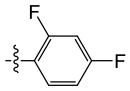	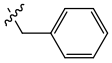	0.079 ± 0.05	>10	29 ± 11
10y	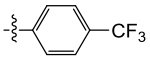	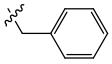	0.041 ± 0.02	>10	>100
10z	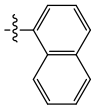	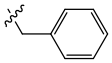	0.057 ± 0.04	>10	21 ± 6
10aa	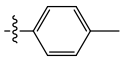		0.030 ± 0.005	>10	2.6 ± 0.5
10bb	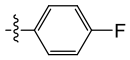		0.0040 ± 0.002	>10	3.1 ± 0.7
10cc	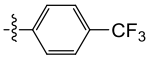		0.038 ± 0.02	8.1 ± 1.4	9.5 ± 1.9
10dd	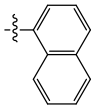		0.018 ± 0.003	7.7 ± 0.6	3.2 ± 0.5
THBNH	--	--	0.2	0.5	NT
RAL	--	--	>10	NT	0.65 ± 0.1
DTG	--	--	>10	NT	0.068 ± 0.01

[a] Concentration of a compound inhibiting the enzymatic function by 50%, expressed as the mean + standard deviation from at least two independent experiments.
[b] NT = not tested.

As for INST, compounds with at least one long wing (**10a-p**) did not show significant inhibition at concentrations up to 100 μM, with the exception of **10d** and **10n**. However, when both C-5 and C-6 positions were occupied by short wings, those with a flexible C-5 wing (**10r** and **10s**)

inhibited INST at submicromolar concentrations. To minimize the undesired INST inhibition, further SAR studies involved only analogues with a short and nonflexible C-5 wing (**10u**-**dd**) to probe the effect of phenyl ring substitution. These analogues consist of two subsets: one with a short and flexible C-6 wing (**10u**-**z**) and one with a short and nonflexible C-6 wing (**10aa**-**dd**). These studies demonstrated again that the combination of two short wings consistently conferred low nanomolar biochemical inhibition against RT RNase H. Particularly notable are analogues with a para-methyl (**10u** and **10aa**) or para-fluoro (**10w** and **10bb**) substituent which exhibited unprecedentedly potent RNase H inhibition (IC_{50} = 0.004–0.030 μM). The IC_{50} of 4 nM with compound **10bb** represents by far the most potent RNase H biochemical inhibition known. In addition, very little inhibition against RT pol was observed with any of these analogues at concentrations up to 10 μM, with the slight exception of **10cc** and **10dd** (pol IC_{50} = 8.1 and 7.7 μM, respectively). Interestingly, the flexibility of the C-6 wing also dramatically impacted the INST inhibition, as compounds with a flexible C-6 wing (**10q, 10u**-**z**) did not inhibit INST significantly (IC_{50} = 21–>100 μM) whereas those with a nonflexible wing (**10t, 10aa**-**dd**) inhibited in the low micromolar range (IC_{50} = 1.5–9.5 μM). Taken together, our biochemical SAR studies confirmed that introducing a second wing at C-5 substantially improves the RNase H inhibitory profile and revealed that the combination of a nonflexible short C-5 wing and a flexible short C-6 wing provides optimized potency and selectivity toward RT RNase H inhibition.

Antiviral Activity. Selected chemotype **10** analogues inhibiting RNase H with extremely high potency and selectivity were further evaluated for their ability to inhibit HIV-1 in an antiviral MAGI assay in parallel with a cytotoxicity assay. This assay measures HIV infection in indicator cells (P4R5) through the expression of a Tat-dependent reporter (β-galactosidase).[32] A total of

twenty three chemotype **10** analogues (**10f**, **10i-dd**) were tested and the results are summarized in Table 2. The most important observation from our antiviral assay was that fifteen out of the twenty three tested analogues inhibited HIV-1 replication in low micromolar range (EC_{50} = 0.6–11.4 μM, Table 2). The exceptions include compounds **10k-n**, which did not inhibit HIV-1 at concentrations up to 20 μM, strongly suggesting that having a long flexible C-6 wing would produce undesired antiviral profile. By contrast, a long nonflexible C-6 wing appeared viable for antiviral activity as shown with compounds **10f**, **10i** and **10j**, and a short C-6 wing was associated with potent antiviral activity, being flexible (**10o, q-r**, **10u-v**) or nonflexible (**10s-t**, **10aa-dd**). On the other hand, the nature of the C-5 wing did not influence the antiviral activity significantly as shown with compounds **10o**, **10p** and **10q**, though most active compounds from the antiviral assay feature short wings at both C-5 and C-6 positions.

Table 2. Antiviral activity of selected chemotype **10** analogues against HIV-1 in the MAGI assay.

Compound	*Antiviral Profile*		*Biochemical Inhibition* [c]		
	EC_{50} [a] *(μM)*	*CC_{50}* [b] *(μM)*	*RNase H IC_{50} (μM)*	*INST IC_{50} (μM)*	*SI* [d]
8	>25	>100	0.25	--	--
10f	6.3 ± 0.5	>100	0.049 ± 0.02	>100	>2.0 x 10^3
10i	1.5 ± 0.003	>100	0.077 ± 0.028	>100	>1.3 x 10^3
10j	3.7 ± 0.2	>100	0.050 ± 0.036	>100	>2.0 x 10^3
10k	>20	ND	0.14 ± 0.09	>100	>0.71 x 10^3
10l	>20	>100	0.11 ± 0.06	>100	>0.91 x 10^3

10m	>20	ND	0.047 ± 0.02	>100	>2.1 x 10^3
10n	>20	ND	0.054 ± 0.02	1.6 ± 0.7	30
10o	15 ± 1.6	54 ± 9	0.12 ± 0.09	>100	>0.83 x 10^3
10p	>20	>100	0.038 ± 0.003	>100	>2.6 x 10^3
10q	6.9 ± 0.2	52 ± 3	0.027 ± 0.002	>100	>3.7 x 10^3
10r	1.4 ± 0.04	>100	0.032 ± 0.006	0.14 ± 0.03	4.4
10s	0.60 ± 0.9	>100	0.056 ± 0.02	0.23 ± 0.04	4.1
10t	6.6 ± 0.9	>100	0.016 ± 0.003	1.5 ± 0.2	94
10u	7.2 ± 1.1	53 ± 3	0.019 ± 0.005	34 ± 8	1.8 x 10^3
10v	8.5 ± 0.5	>100	0.054 ± 0.037	>100	>1.9 x 10^3
10w	>20	>100	0.019 ± 0.003	71 ± 33	3.7 x 10^3
10x	>20	>100	0.079 ± 0.050	29 ± 11	0.37 x 10^3
10y	>20	>100	0.041 ± 0.023	>100	>2.4 x 10^3
10z	>20	>100	0.057 ± 0.039	21 ± 6	0.37 x 10^3
10aa	4.5 ± 0.1	>100	0.030 ± 0.005	2.6 ± 0.5	87
10bb	6.1 ± 0.4	58.4 ± 0.8	0.0040 ± 0.002	3.1 ± 0.7	0.78 x 10^3
10cc	3.5 ± 0.2	>100	0.038 ± 0.016	9.5 ± 1.9	0.25 x 10^3
10dd	11.4 ± 0.6	76.8 ± 3.4	0.018 ± 0.003	3.2 ± 0.5	0.18 x 10^3
RAL	0.03	NT	>10	0.65 ± 0.14	<0.065

DTG	0.02	NT	>10	0.068 ± 0.01	<0.0068

[a] Concentration of a compound inhibiting HIV-1 replication by 50%, expressed as the mean + standard deviation from at least two independent experiments.

[b] Concentration of a compound causing 50% cytotoxicity, expressed as the mean + standard deviation from at least two independent experiments.

[c] Significant RT pol inhibition was not observed against any of these compounds (pol IC_{50}s >7.7 μM).

[d] Biochemical selective index, defined as INST IC_{50} / RNase H IC_{50}.

To demonstrate the potential correlation between the observed antiviral activity and the biochemical targets, the IC_{50}s for inhibition against RNase H and INST, and the biochemical selective index, are also listed in Table 2. Inhibition against RT pol is generally lacking at concentrations up to 7.7 μM, and thus not listed. Interestingly, although the analogue with nanomolar antiviral activity (**10s**) inhibited both RNase H and INST potently, the biochemical inhibition still favored RNase H over INST by a large margin (~4 fold). In fact the vast majority of the analogues active in our antiviral assay showed either no INST inhibition at 100 μM (**10f**, **10i-j**, **10o-q**, **10v**) or highly selective (>87 fold selectivity) RNase H inhibition over INST inhibition (**10u**, **10aa-dd**). Compound **10n** represents a rare exception where potent inhibition against RNase H (IC_{50} = 0.054 μM) and INST (IC_{50} = 1.6 μM) did not confer significant antiviral activity (EC_{50} > 20 μM). Importantly, neither of the two INSTIs, RAL and DTG, inhibited RNase H in our biochemical assay at concentrations up to 10 μM, suggesting that our RNase H biochemical assay is selective. All these observations are in line with RNase H inhibition as the potential antiviral mechanism of action. Notably, compared with the ultra-potent RNase H inhibition (low nanomolar), the level of HIV-1 inhibition was moderate (low micromolar to submicromolar). This may reflect the underlying challenge for small molecule inhibitors to compete against the tight binding substrate. Nevertheless, considering that the

single-winged chemotype **8** did not inhibit HIV-1 at 25 μM, the consistent antiviral activity observed with the new double-winged chemotype **10** represents a major improvement and suggests that carefully designed active site inhibitors of RNase H could cut into the substrate dominance and confer antiviral activity. As far as cytotoxicity is concerned, with the exception of the mild cytotoxicity associated with **10o** (CC_{50} = 54 μM)**, 10q** (CC_{50} = 52 μM)**, 10u** (CC_{50} =53 μM), **10bb** (CC_{50} = 58 μM) and **10dd** (CC_{50} = 77 μM), no appreciable cytotoxicity was observed with chemotype **10** analogues at concentrations up to 100 μM.

Conclusions. Based on a previously reported HPD subtype **8** that potently and selectively inhibited RNase H without inhibiting HIV-1 in cell culture, we have redesigned a new double-winged HPD chemotype **10** featuring an additional wing at the C-5 position. The biochemical assays showed that drastically improved RNase H inhibition was achieved when both wings were short and that the low nanomolar RNase H inhibition was largely selective over RT pol and INST inhibition. Most importantly, antiviral activity was observed against HIV-1 with these double winged analogues at submicromolar to low micromolar concentrations. The antiviral potency appeared to be correlated with the ultra-potent RNase H biochemical inhibition. Further biophysical and mechanistic studies are currently underway and will be reported in due course. Nevertheless, the medicinal chemistry reported herein suggests that ultra-potent RNase H inhibitors could confer significant antiviral activity.

Experimental

Chemistry

General Procedures. All commercial chemicals were used as supplied unless otherwise indicated. Dry solvents were either purchased (toluene and MeOH) or dispensed under argon from an anhydrous solvent system with two packed columns of neutral alumina or molecular sieves. Flash chromatography was performed on a Teledyne Combiflash RF-200 with RediSep columns (silica) and indicated mobile phase. All moisture sensitive reactions were performed under an inert atmosphere of ultra-pure argon with oven-dried glassware. ^{1}H and ^{13}C NMR spectra were recorded on a Varian 600 MHz spectrometer. Mass data were acquired on an Agilent TOF II TOS/MS spectrometer capable of ESI and APCI ion sources. Analysis of sample purity was performed on a Varian Prepstar SD-1 HPLC system with a Phenomenex Gemini, 5 micron C18 column (250mm x 4.6 mm). HPLC conditions**:** solvent A = H_2O containing 0.1% TFA, solvent B = MeCN; flow rate = 1.0 mL/min; compounds were eluted with a gradient of 20% MeCN/H_2O to 100% MeCN for 30 min. Purity was determined by total absorbance at 254 nm. All tested compounds have a purity ≥ 95%.

General procedure 1 for debenzylation via hydrogenation (10a-10dd). To a solution of compound **16** (100 mg) in MeOH (7.0 mL) was added Pd/C (20 mg, 10%) and the reaction mixture was degassed and purged with H_2 for three times. The reaction vessel was shaken under H_2 (40-50 psi) atmosphere at room temperature for appropriate time. The reaction was monitored by both TLC and MS. The reaction mixture was filtered through a short pad of celite, washed with MeOH and the solvent was removed *in vacco*. The solid obtained was further purified by trituration with MeOH, ethyl acetate and DCM furnished pure compounds **10a-10dd** as solid.

General procedure 2 for TFA-mediated debenzylation (10a-10dd). To a microwave reaction vessel were added compound **16** (0.26 mmol) and TFA (6~10 mL). The reaction vessel was irradiated at 120 °C for the appropriate time. The reaction was monitored by TLC and MS. The

reaction mixture was transferred to a round-bottom flask to remove the solvent under reduced pressure. The crude product was purified by flash chromatography on C18 reverse phase column (H_2O-MeOH) or trituration with MeOH, ethyl acetate and DCM yielded pure compounds **10a-10dd** as solid.

***N*-([1,1'-Biphenyl]-4-yl)-6-([1,1'-biphenyl]-4-ylamino)-3-hydroxy-2,4-dioxo-1,2,3,4-tetrahydropyrimidine-5-carboxamide (10a).** Yield 48%. ^{1}H NMR (600 MHz, DMSO-d_6) δ 12.52 (s, 1H), 12.17 (s, 1H), 10.45 (s, 1H), 7.76-7.66 (m, 10H), 7.65-7.60 (m, 6H) 7.50-7.35 (m, 2H); ^{13}C NMR (150 MHz, DMSO-d_6) δ 166.2, 162.1, 139.5, 139.3, 137.7, 135.0, 129.0, 128.8, 127.6, 127.5, 127.1, 127.0, 126.5, 126.2, 125.4, 120.2, 81.3; HRMS-ESI(-) *m/z* calcd for $C_{29}H_{21}N_4O_4$ 489.1563 $[M-H]^-$, found 489.1563.

6-([1,1'-Biphenyl]-4-ylamino)-*N*-(4'-fluoro-[1,1'-biphenyl]-4-yl)-3-hydroxy-2,4-dioxo-1,2,3,4-tetrahydropyrimidine-5-carboxamide (10b). Yield 43%. ^{1}H NMR (600 MHz, DMSO-d_6) δ 12.51 (s, 1H), 12.06 (s, 1H), 10.46 (s, 1H), 7.76-7.62 (m, 11H), 7.47-7.44 (m, 4H), 7.37-7.36 (m, 1H), 7.26-7.25 (s, 1H); ^{13}C NMR (150 MHz, DMSO-d_6) δ 166.1, 162.4, 160.8, 154.4, 146.9, 139.3, 138.3, 137.6, 136.0, 134.9, 134.1, 129.0, 128.9, 128.2, 128.1, 127.7, 127.5, 127.1, 126.5, 126.2, 125.6, 120.3, 115.7, 115.5, 81.2; HRMS-ESI(-) *m/z* calcd for $C_{29}H_{20}FN_4O_4$ 507.1469 $[M-H]^-$, found 507.1492.

6-([1,1'-Biphenyl]-4-ylamino)-3-hydroxy-*N*-(4'-methoxy-[1,1'-biphenyl]-4-yl)-2,4-dioxo-1,2,3,4-tetrahydropyrimidine-5-carboxamide (10c). Yield 54%. ^{1}H NMR (600 MHz, DMSO-d_6) δ 12.52 (s, 1H), 12.00 (s, 1H), 10.42 (s, 1H), 7.74-7.58 (m, 11H), 7.47-7.37 (m, 4H), 6.99-6.98 (m, 2H); ^{13}C NMR (150 MHz, DMSO-d_6) δ 166.0, 162.0, 158.6, 154.3, 146.8, 139.3, 138.4, 136.9, 134.9, 134.9, 132.0, 129.0, 127.7, 127.5, 127.3, 126.6, 126.5, 125.7, 120.3, 114.3, 81.2, 55.1; HRMS-ESI(-) *m/z* calcd for $C_{30}H_{23}N_4O_5$ 519.1668 $[M-H]^-$, found 519.1688.

***N*-Benzyl-1-(hydroxy)-1,2,3,6-tetrahydro-2,6-dioxo-4-(biphenylamino)pyrimidine-5-carboxamide (10d).** Yield 77%. ^{1}H NMR (600 MHz, DMSO-d_6) δ 12.76 (s, 1H), 11.33 (s, 1H), 10.34 (s, 1H), 10.04 (dd, J = 6.0, 4.8 1H), 7.74-7.20 (m, 14H), 4.50 (d, J = 5.4, 2H); ^{13}C NMR (150 MHz, DMSO-d_6) δ 167.7, 161.6, 154.0, 147.0, 139.3, 138.1, 135.2, 129.0, 128.4, 127.7, 127.5, 127.2, 126.9, 126.5, 125.4, 80.9, 41.9; HRMS-ESI(-) *m/z* calcd for $C_{24}H_{20}N_4O_4$ 427.1412 $[M-H]^-$, found 427.1414.

***N*-(4-Fluorobenzyl)-1-(hydroxy)-1,2,3,6-tetrahydro-2,6-dioxo-4-(biphenylamino)pyrimidine-5-carboxamide (10e).** Yield 19%. ^{1}H NMR (600 MHz, DMSO-d_6) δ 12.73 (s, 1H), 11.32 (s, 1H), 10.33 (s, 1H), 10.04 (t, J = 6.0, 1H), 7.74-7.15 (m, 13H), 4.48 (d, J = 6.0, 2H); ^{13}C NMR (150 MHz, DMSO-d_6) δ 167.8, 161.6, 161.2 (d, J_{CF} = 240.8 Hz), 154.0, 147.0, 139.3, 138.1, 135.6 (d, J_{CF} = 3.2 Hz), 135.2, 129.2 (d, J_{CF} = 7.7 Hz), 129.0, 127.7, 127.5, 126.5, 125.4, 115.1 (d, J_{CF} = 20.6 Hz), 80.9, 41.1; HRMS-ESI(-) *m/z* calcd for $C_{24}H_{19}FN_4O_4$ 445.1318 $[M-H]^-$, found 445.1324.

***N*-(3-Fluorobenzyl)-1-(hydroxy)-1,2,3,6-tetrahydro-2,6-dioxo-4 (biphenylamino)pyrimidine-5-carboxamide (10f).** Yield 21%. ^{1}H NMR (600 MHz, DMSO-d_6) δ 12.67 (s, 1H), 10.32 (s, 1H), 10.06 (t, J = 6.0, 1H), 7.72-7.07 (m, 13H), 4.50 (d, J = 6.0, 2H); ^{13}C NMR (150 MHz, DMSO-d_6) δ 167.8, 162.2 (d, J_{CF} = 241.8 Hz), 161.6, 154.0, 147.0, 142.6 (d, J_{CF} = 6.6 Hz), 139.3, 138.1, 135.2, 130.3 (d, J_{CF} = 7.7 Hz), 129.0, 127.7, 127.5, 126.9, 126.5, 125.4, 123.2 (d, J_{CF} = 3.6 Hz), 113.8 (d, J_{CF} = 21.8 Hz), 113.6 (d, J_{CF} = 20.7 Hz), 80.9, 41.4; HRMS-ESI(-) *m/z* calcd for $C_{24}H_{19}FN_4O_4$ 445.1318 $[M-H]^-$, found 445.1315.

***N*-(2-Fluorobenzyl)-1-(hydroxy)-1,2,3,6-tetrahydro-2,6-dioxo-4-(biphenylamino)pyrimidine-5-carboxamide (10g).** Yield 48%. ^{1}H NMR (600 MHz, DMSO-d_6) δ 12.67 (s, 1H), 11.35 (br s, 1H), 10.35 (s, 1H), 10.05 (dd, J = 6.0, 5.4, 1H), 7.74-7.17 (m,

13H), 4.54 (d, J = 5.4, 2H); ^{13}C NMR (150 MHz, DMSO-d_6) δ 167.7, 161.6, 160.2 (d, J_{CF} = 242.9 Hz), 154.0, 146.97, 139.3, 138.1, 135.1, 129.5 (d, J_{CF} = 4.3 Hz), 129.0 (d, J_{CF} = 10.8 Hz), 129.0, 127.7, 127.5, 126.5, 126.1 (d, J_{CF} = 11.1 Hz), 125.4, 124.4 (d, J_{CF} = 3.3 Hz), 115.2 (d, J_{CF} = 20.6 Hz), 80.9, 36.0; HRMS-ESI(-) *m/z* calcd for $C_{24}H_{19}FN_4O_4$ 445.1318 [M-H]-, found 445.1324.

***N*-(3-Chloro-2-fluorobenzyl)-1-(hydroxy)-1,2,3,6-tetrahydro-2,6-dioxo-4-(biphenylamino)pyrimidine-5-carboxamide (10h).** Yield 25%. ^{1}H NMR (600 MHz, DMSO-d_6) δ 12.60 (s, 1H), 11.37 (br s, 1H), 10.35 (s, 1H), 10.10 (dd, J = 6.0, 5.4 Hz, 1H), 7.73-7.20 (m, 12H), 4.57 (d, J = 6.0 Hz, 2H); ^{13}C NMR (150 MHz, DMSO-d_6) δ 167.8, 161.6, 155.2 (d, J_{CF} = 246 Hz), 154.1, 147.0, 139.3, 138.1, 135.1, 129.2, 129.0, 128.4 (d, J_{CF} = 10.4 Hz), 128.3 (d, J_{CF} = 3.4 Hz), 127.7, 127.5, 126.5, 125.4, 125.3 (d, J_{CF} = 4.5 Hz), 119.5 (d, J_{CF} = 17.3 Hz), 80.9, 36.1 (d, J_{CF} = 3.5 Hz); HRMS-ESI(-) *m/z* calcd for $C_{24}H_{18}ClFN_4O_4$ 479.0928 $[M-H]^-$, found 479.0931.

***N*-(2,4-Difluorobenzyl)-1-(hydroxy)-1,2,3,6-tetrahydro-2,6-dioxo-4-(biphenylamino) pyrimidine-5-carboxamide (10i).** Yield 55%. ^{1}H NMR (600 MHz, DMSO-d_6) δ 12.64 (s, 1H), 11.35 (br s, 1H), 10.34 (s,1H), 10.04 (s, 1H), 7.73-7.07 (m, 12H), 4.50 (d, J = 5.4 Hz, 2H); ^{13}C NMR (150 MHz, DMSO-d_6) δ 168.2, 162.7, 162.0, 159.8, 156.8, 154.5, 147.4, 139.8, 138.6, 135.5, 131.3, 129.4, 128.1, 127.9, 126.9, 125.9, 123.0, 122.9, 111.9, 111.8, 104.4, 104.0, 81.3, 36.0; HRMS-ESI(-) *m/z* calcd for $C_{24}H_{18}F_2N_4O_4$ 463.1223 $[M-H]^-$, found 463.1230.

***N*-(2,5-Difluorobenzyl)-1-(hydroxy)-1,2,3,6-tetrahydro-2,6-dioxo-4-(biphenylamino) pyrimidine-5-carboxamide (10j).** Yield 84%. ^{1}H NMR (600 MHz, DMSO-d_6) δ 12.59 (s, 1H), 11.35 (br s, 1H), 10.35 (s,1H), 10.07 (t, J = 6.0 Hz, 1H), 7.73-7.68 (m, 4H), 7.48-7.37 (m, 5H), 7.26-7.15 (m, 3H), 4.53 (d, J = 5.4 Hz, 2H); ^{13}C NMR (150 MHz, DMSO-d_6) δ 168.3, 162.0,

159.3, 157.7, 154.5, 147.4, 139.8, 138.6, 135.5, 129.4, 128.1, 127.9, 126.9, 125.9, 117.2, 116.2, 115.6, 115.5, 81.3, 36.3; HRMS-ESI(-) *m/z* calcd for $C_{24}H_{18}F_2N_4O_4$ 463.1223 $[M-H]^-$, found 463.1227.

***N*-([1,1'-Biphenyl]-4-yl)-6-(([1,1'-biphenyl]-4-ylmethyl)amino)-3-hydroxy-2,4-dioxo-1,2,3,4-tetrahydropyrimidine-5-carboxamide (10k).** Yield 92%. ^{1}H NMR (DMSO-d_6, 600 MHz) δ 12.00 (s, 1H), 11.28 (s, 1H), 10.72 (s, 1H), 7.70 (d, J = 8.4 Hz, 2H), 7.67 (d, J = 7.8 Hz, 2H), 7.63-7.59 (m, 6H), 7.46-7.40 (m, 6H), 7.37-7.34 (m, 1H), 7.30 (t, J = 6.6 Hz, 1H), 4.74 (d, J = 5.4 Hz, 2H); ^{13}C NMR (DMSO-d_6, 150 MHz) δ 166.7, 162.3, 155.8, 147.7, 140.2, 140.1, 140.0, 138.3, 136.5, 129.4, 129.3, 128.5, 127.9, 127.5, 127.5, 127.4, 127.1, 126.6, 120.6, 80.2, 44.9; HRMS-ESI(-) *m/z* calcd for $C_{30}H_{23}N_4O_4$ 503.1719 $[M-H]^-$, found 503.1735.

***N*-([1,1'-Biphenyl]-4-yl)-6-(([1,1'-biphenyl]-4-ylmethyl)amino)-3-hydroxy-2,4-dioxo-1,2,3,4-tetrahydropyrimidine-5-carboxamide (10l).** Yield 76%. ^{1}H NMR (DMSO-d_6, 600 MHz) δ 11.42 (s, 1H), 10.23 (s, 1H), 9.99 (s, 1H), 7.67-7.58 (m, 8H), 7.45-7.41 (m, 4H), 7.40 (d, J = 7.8 Hz, 1H), 7.35-7.32 (m, 4H), 4.67 (d, J = 5.4 Hz, 2H), 4.45 (d, J = 6.0 Hz, 2H); ^{13}C NMR (DMSO-d_6, 150 MHz) δ 168.3, 161.9, 155.6, 147.9, 140.3, 140.1, 139.9, 139.3, 139.2, 136.7, 129.4, 129.3, 128.4, 128.2, 128.2, 127.9, 127.7, 127.5, 127.2, 127.1, 127.0, 79.8, 44.7, 41.8; HRMS-ESI(-) *m/z* calcd for $C_{31}H_{25}N_4O_4$ 517.1876 $[M-H]^-$, found 517.1889.

6-(([1,1'-Biphenyl]-4-ylmethyl)amino)-3-hydroxy-2,4-dioxo-N-phenyl-1,2,3,4-tetrahydropyrimidine-5-carboxamide (10m). Yield 79%. ^{1}H NMR (DMSO-d_6, 600 MHz) δ 11.93 (s, 1H), 11.18 (s, 1H), 10.32 (s, 1H), 7.68-7.64 (m, 4H), 7.52 (d, J = 8.4 Hz, 2H), 7.46-7.41 (m, 4H), 7.36-7.34 (m, 1H), 7.27 (t, J = 7.8 Hz, 2H), 7.01 (t, J = 7.2 Hz, 1H), 4.72 (d, J = 5.4 Hz, 2H); ^{13}C NMR (DMSO-d_6, 150 MHz) δ 169.1, 161.8, 144.1, 129.4, 129.3, 128.4, 127.9, 127.5,

127.1, 120.2, 117.3, 110.0, 80.2, 31.1; HRMS-ESI(-) *m/z* calcd for $C_{24}H_{19}N_4O_4$ 427.1406 $[M-H]^-$, found 427.1433.

6-(([1,1'-Biphenyl]-4-ylmethyl)amino)-*N*-benzyl-3-hydroxy-2,4-dioxo-1,2,3,4-tetrahydropyrimidine-5-carboxamide (10n). Yield 81%. ^{1}H NMR (DMSO-d_6, 600 MHz) δ 11.45 (s, 1H), 11.38 (s, 1H), 10.23 (s, 1H), 9.94 (s, 1H), 7.67-7.64 (m, 4H), 7.44 (t, J = 7.8 Hz, 2H), 7.39 (d, J = 7.8 Hz, 2H), 7.36-7.29 (m, 3H), 7.26 (d, J = 7.8 Hz, 2H), 7.21 (t, J = 7.8 Hz, 1H), 4.67 (d, J = 6.0 Hz, 2H), 4.41 (d, J = 5.4 Hz, 2H); ^{13}C NMR (DMSO-d_6, 150 MHz) δ 168.2, 161.8, 155.4, 147.7, 140.0, 139.9, 139.8, 136.6, 129.4, 128.8, 128.4, 127.9, 127.5, 127.5, 127.4, 127.2, 127.0, 79.7, 44.8, 42.1; HRMS-ESI(-) *m/z* calcd for $C_{25}H_{21}N_4O_4$ 441.1563 $[M-H]^-$, found 441.1591.

***N*-([1,1'-Biphenyl]-4-yl)-6-(benzylamino)-3-hydroxy-2,4-dioxo-1,2,3,4-tetrahydropyrimidine-5-carboxamide (10o).** Yield 86%. ^{1}H NMR (DMSO-d_6, 600 MHz) δ 12.00 (s, 1H), 11.22 (s, 1H), 10.38 (s, 1H), 7.63-7.59 (m, 7H), 7.43-7.38 (m, 4H), 7.34-7.30 (m, 3H), 4.68 (d, J = 5.4 Hz, 2H); ^{13}C NMR (DMSO-d_6, 150 MHz) δ 166.7, 162.3, 155.8, 152.8, 147.7, 140.3, 140.0, 139.6, 138.3, 137.4, 135.3, 134.0, 129.3, 129.2, 128.1, 127.8, 127.5, 127.5, 127.4, 127.2, 126.6, 126.5, 120.6, 119.0, 80.2, 45.2; HRMS-ESI(-) *m/z* calcd for $C_{24}H_{19}N_4O_4$ 427.1406 $[M-H]^-$, found 427.1434.

***N*-([1,1'-Biphenyl]-4-ylmethyl)-6-(benzylamino)-3-hydroxy-2,4-dioxo-1,2,3,4-tetrahydropyrimidine-5-carboxamide (10p).** Yield 78%. ^{1}H NMR (DMSO-d_6, 600 MHz) δ 11.41 (s, 1H), 11.32 (s, 1H), 10.23 (s, 1H), 9.96 (s, 1H), 7.61-7.57 (m, 4H), 7.43-7.40 (m, 2H), 7.36-7.28 (m, 8H), 4.61 (d, J = 4.8 Hz, 2H), 4.43 (d, J = 4.8 Hz, 2H); ^{13}C NMR (DMSO-d_6, 150 MHz) δ 168.2, 161.8, 155.3, 147.7, 140.3, 139.2, 137.4, 129.3, 129.2, 128.2, 128.1, 128.0, 127.8,

127.7, 127.1, 127.0, 79.7, 45.1, 41.8; HRMS-ESI(-) *m/z* calcd for $C_{25}H_{21}N_4O_4$ 441.1563 $[M-H]^-$, found 441.1588.

6-(Benzylamino)-3-hydroxy-2,4-dioxo-*N*-phenyl-1,2,3,4-tetrahydropyrimidine-5-carboxamide (10q). Yield 84%. ^{1}H NMR (DMSO-d_6, 600 MHz) δ 12.03 (s, 1H), 11.88 (s, 1H), 11.33-11.31 (m, 1H), 10.39 (s, 1H), 7.51-7.48 (m, 2H), 7.39-7.37 (m, 2H), 7.34-7.25 (m, 5H), 7.03-7.00 (m, 1H), 4.67 (d, J = 6.0 Hz, 2H); ^{13}C NMR (DMSO-d_6, 150 MHz) δ 167.0, 166.7, 165.2, 162.3, 157.9, 155.7, 149.1, 147.6, 138.9, 138.8, 137.3, 129.3, 128.1, 127.8, 123.7, 123.5, 120.2, 80.2, 45.3; HRMS-ESI(-) *m/z* calcd for $C_{18}H_{15}N_4O_4$ 351.1093 $[M-H]^-$, found 351.1126.

***N*-Benzyl-6-(benzylamino)-3-hydroxy-2,4-dioxo-1,2,3,4-tetrahydropyrimidine-5-carboxamide (10r).** Yield 83%. ^{1}H NMR (DMSO-d_6, 600 MHz) δ 11.42 (s, 1H), 11.33 (s, 1H), 10.22 (s, 1H), 9.92 (s, 1H), 7.38-7.36 (m, 2H), 7.30-7.29 (m, 5H), 7.25-7.21 (m, 3H), 4.61 (d, J = 6.0 Hz, 2H), 4.40 (d, J = 6.0 Hz, 2H); ^{13}C NMR (DMSO-d_6, 150 MHz) δ 181.5, 168.2, 161.8, 155.4, 147.7, 139.9, 137.4, 129.2, 128.8, 128.0, 127.8, 127.6, 127.5, 127.2, 96.2, 79.7, 45.1, 42.1; HRMS-ESI(-) *m/z* calcd for $C_{19}H_{17}N_4O_4$ 365.1250 $[M-H]^-$, found 365.1292.

***N*-Benzyl-1-(hydroxy)-1,2,3,6-tetrahydro-2,6-dioxo-4-(phenylamino)pyrimidine-5-carboxamide (10s).** Yield 50%. ^{1}H NMR (600 MHz, DMSO-d_6) δ 12.72 (s, 1H), 11.26 (s, 1H), 10.32 (s, 1H), 10.03 (t, J = 2.4, 1H), 7.43-7.26 (m, 10H), 4.49 (s, 2H); ^{13}C NMR (150 MHz, DMSO-d_6) δ 167.7, 161.6, 154.0, 147.0, 139.3, 135.8, 129.5, 128.4, 127.2, 126.9, 126.5, 124.9, 81.7, 41.9; HRMS-ESI(-) *m/z* calcd for $C_{18}H_{16}N_4O_4$ 351.1099 $[M-H]^-$, found 351.1103.

3-Hydroxy-2,4-dioxo-*N*-phenyl-6-(phenylamino)-1,2,3,4-tetrahydropyrimidine-5-carboxamide (10t). Yield 87%. ^{1}H NMR (DMSO-d_6, 600 MHz) δ 12.33 (s, 1H), 12.27 (s, 1H), 9.96 (s, 1H), 7.55 (d, J = 7.8 Hz, 2H), 7.52 (d, J = 6.0 Hz, 2H), 7.32-7.27 (m, 3H), 7.13-6.96 (m,

3H); ^{13}C NMR (DMSO-d_6, 150 MHz) δ 167.3, 165.0, 163.4, 139.4, 129.4, 129.3, 123.2, 120.1, 110.0; HRMS-ESI(-) *m/z* calcd for $C_{17}H_{13}N_4O_4$ 337.0937 $[M-H]^-$, found 337.0961.

6-(Benzylamino)-3-hydroxy-2,4-dioxo-*N*-(*p*-tolyl)-1,2,3,4-tetrahydropyrimidine-5-carboxamide (10u). Yield 79%. ^{1}H NMR (DMSO-d_6, 600 MHz) δ 11.89 (s, 1H), 11.01 (s, 1H), 10.08 (s, 1H), 7.38-7.34 (m, 4H), 7.31-7.28 (m, 3H), 7.06 (d, J = 7.8 Hz, 2H), 4.63 (d, J = 5.4 Hz, 2H), 2.21 (s, 3H); ^{13}C NMR (DMSO-d_6, 150 MHz) δ 166.7, 163.4, 162.4, 138.0, 136.6, 132.2, 129.6, 129.2, 129.1, 127.8, 120.1, 110.0, 80.3, 44.9, 20.83; HRMS-ESI(-) *m/z* calcd for $C_{19}H_{17}N_4O_4$ 365.1250 $[M-H]^-$, found 365.1273.

6-(Benzylamino)-*N*-(4-ethylphenyl)-3-hydroxy-2,4-dioxo-1,2,3,4-tetrahydropyrimidine-5-carboxamide (10v). Yield 83%. ^{1}H NMR (DMSO-d_6, 600 MHz) δ 11.80 (s, 1H), 11.41 (s, 1H), 11.23 (s, 1H), 10.34 (s, 1H), 7.40-7.36 (m, 4H), 7.32-7.29 (m, 3H), 7.10-7.09 (m, 2H), 4.64 (d, J = 5.4 Hz, 2H), 2.50 (q, J = 1.4 Hz, J = 7.5 Hz, 2H), 1.11 (t, J = 7.8 Hz, 3H); ^{13}C NMR (DMSO-d_6, 150 MHz) δ 166.5, 162.2, 155.7, 147.6, 139.0, 137.4, 136.5, 129.2, 128.5, 128.0, 127.8, 120.3, 80.0, 45.2, 27.9, 16.1; HRMS-ESI(-) *m/z* calcd for $C_{20}H_{19}N_4O_4$ 379.1406 $[M-H]^-$, found 379.1430.

6-(Benzylamino)-*N*-(4-fluorophenyl)-3-hydroxy-2,4-dioxo-1,2,3,4-tetrahydropyrimidine-5-carboxamide (10w). Yield 78%. ^{1}H NMR (DMSO-d_6, 600 MHz) δ 11.95 (s, 1H), 11.42 (s, 1H), 10.96 (s, 1H), 10.15 (s, 1H), 7.52-7.50 (m, 2H), 7.37-7.34 (m, 2H), 7.31-7.28 (m, 3H), 7.08 (t, J = 9.0 Hz, 1H), 4.63 (d, J = 6.0 Hz, 2H); ^{13}C NMR (DMSO-d_6, 150 MHz) δ 166.8, 162.4, 159.1, 157.5, 137.9, 135.4, 129.1, 127.9, 127.8, 121.9, 121.9, 115.8, 115.7, 80.2, 45.0; HRMS-ESI(-) *m/z* calcd for $C_{18}H_{14}FN_4O_4$ 369.0999 $[M-H]^-$, found 369.1115.

6-(Benzylamino)-*N*-(2,4-difluorophenyl)-3-hydroxy-2,4-dioxo-1,2,3,4-tetrahydropyrimidine-5-carboxamide (10x). Yield 86%. ^{1}H NMR (DMSO-d_6, 600 MHz) δ

12.03 (s, 1H), 11.49 (s, 1H), 11.04 (s, 1H), 10.40 (s, 1H), 8.20-8.16 (m, 1H), 7.38-7.31 (m, 6H), 6.99 (t, *J* = 8.4 Hz, 1H), 4.66 (d, *J* = 5.4 Hz, 2H); ^{13}C NMR (DMSO-*d*$_6$, 150 MHz) δ 166.7, 162.4, 159.7, 155.8, 153.5, 137.3, 129.2, 128.1, 127.8, 123.0, 110.0, 80.1, 45.2; HRMS-ESI(-) *m/z* calcd for $C_{18}H_{13}F_2N_4O_4$ 387.0905 $[M-H]^-$, found 387.0926.

6-(Benzylamino)-3-hydroxy-2,4-dioxo-*N*-(4-(trifluoromethyl)phenyl)-1,2,3,4-tetrahydropyrimidine-5-carboxamide (10y). Yield 81%. ^{1}H NMR (DMSO-*d*$_6$, 600 MHz) δ 12.31 (s, 1H), 10.83 (s, 1H), 10.21 (s, 1H), 7.72 (d, *J* = 7.8 Hz, 2H), 7.60 (d, *J* = 8.4 Hz, 2H), 7.37-7.35 (m, 2H), 7.32-7.28 (m, 3H), 4.64 (d, *J* = 4.8 Hz, 2H); ^{13}C NMR (DMSO-*d*$_6$, 150 MHz) δ 167.2, 162.6, 157.3, 142.7, 137.9, 129.1, 127.9, 127.8, 126.5, 125.8, 119.8, 80.4, 45.3, 20.8; HRMS-ESI(-) *m/z* calcd for $C_{19}H_{14}F_3N_4O$ 419.0967 $[M-H]^-$, found 419.1002.

6-(Benzylamino)-3-hydroxy-*N*-(naphthalen-1-yl)-2,4-dioxo-1,2,3,4-tetrahydropyrimidine-5-carboxamide (10z). Yield 78%. ^{1}H NMR (DMSO-*d*$_6$, 600 MHz) δ 13.19 (s, 1H), 10.02 (s, 1H), 8.37 (d, *J* = 7.2 Hz, 1H), 8.25 (d, *J* = 8.4 Hz, 1H), 8.15 (s, 1H), 7.87 (d, *J* = 7.8 Hz, 1H), 7.54 (t, *J* = 7.8 Hz, 1H), 7.51-7.48 (m, 2H), 7.37 (t, *J* = 8.4 Hz, 1H), 7.31-7.30 (m, 3H), 7.22-7.20 (m, 1H), 4.56 (d, *J* = 4.8 Hz, 2H); ^{13}C NMR (DMSO-*d*$_6$, 150 MHz) δ 168.1, 165.1, 164.0, 162.6, 154.1, 140.8, 135.7, 134.1, 128.9, 128.7, 127.1, 127.0, 126.4, 126.2, 126.1, 125.5, 122.1, 121.5, 116.3, 82.2, 43.7; HRMS-ESI(-) *m/z* calcd for $C_{22}H_{17}N_4O_4$ 401.1250 $[M-H]^-$, found 401.1277.

3-Hydroxy-2,4-dioxo-6-(phenylamino)-*N*-(*p*-tolyl)-1,2,3,4-tetrahydropyrimidine-5-carboxamide (10aa). Yield 83%. ^{1}H NMR (DMSO-*d*$_6$, 600 MHz) δ 12.36 (s, 1H), 12.17 (s, 1H), 9.94 (s, 1H), 7.51 (d, *J* = 7.2 Hz, 2H), 7.44 (d, *J* = 7.8 Hz, 2H), 7.31 (t, *J* = 7.8 Hz, 2H), 7.09 (d, *J* = 7.8 Hz, 3H), 2.23 (s, 3H); ^{13}C NMR (DMSO-*d*$_6$, 150 MHz) δ 167.1, 163.0, 136.8, 132.1, 129.7, 129.5, 129.4, 123.1, 120.1, 118.6, 82.0, 20.8; HRMS-ESI(-) *m/z* calcd for $C_{18}H_{15}N_4O_4$ 351.1093 $[M-H]^-$, found 351.1125.

***N*-(4-Fluorophenyl)-3-hydroxy-2,4-dioxo-6-(phenylamino)-1,2,3,4-tetrahydropyrimidine-5-carboxamide (10bb).** Yield 89%. ^{1}H NMR (DMSO-d_6, 600 MHz) δ 12.29 (s, 1H), 12.22 (s, 1H), 9.92 (s, 1H), 7.58-7.56 (m, 2H), 7.50 (d, J = 6.6 Hz, 2H), 7.32 (t, J = 7.8 Hz, 2H), 7.12 (t, J = 7.8 Hz, 3H); ^{13}C NMR (DMSO-d_6, 150 MHz) δ 167.1, 163.0, 159.0, 157.4, 155.9, 135.6, 129.4, 123.3, 121.9, 115.9, 115.7, 110.0, 93.8, 80.8; HRMS-ESI(-) *m/z* calcd for $C_{17}H_{12}FN_4O_4$ 355.0843 $[M-H]^-$, found 355.0880.

3-Hydroxy-2,4-dioxo-6-(phenylamino)-*N*-(4-(trifluoromethyl)phenyl)-1,2,3,4-tetrahydropyrimidine-5-carboxamide (10cc). Yield 84%. ^{1}H NMR (DMSO-d_6, 600 MHz) δ 12.46 (s, 1H), 12.21 (s, 1H), 10.18 (s, 1H), 7.79 (d, J = 8.4 Hz, 2H), 7.65 (d, J = 8.4 Hz, 2H), 7.46 (d, J = 7.8 Hz, 2H), 7.36 (t, J = 7.2 Hz, 2H), 7.19-7.17 (m, 1H); ^{13}C NMR (DMSO-d_6, 150 MHz) δ 167.3, 162.9, 142.7, 129.7, 126.6, 125.7, 124.2, 123.4, 120.0, 110.0, 81.8; HRMS-ESI(-) *m/z* calcd for $C_{18}H_{12}F_3N_4O_4$ 405.0811 $[M-H]^-$, found 405.0847.

3-Hydroxy-*N*-(naphthalen-1-yl)-2,4-dioxo-6-(phenylamino)-1,2,3,4-tetrahydropyrimidine-5-carboxamide (10dd). Yield 80%. ^{1}H NMR (DMSO-d_6, 600 MHz) δ 12.60 (s, 1H), 12.50 (s, 1H), 10.54 (s, 1H), 8.27 (d, J = 7.2 Hz, 1H), 8.15 (d, J = 8.4 Hz, 1H), 7.95 (d, J = 7.8 Hz, 1H), 7.69 (d, J = 8.4 Hz, 1H), 7.63 (t, J = 7.2 Hz, 1H), 7.55 (t, J = 7.2 Hz, 1H), 7.48 (t, J = 7.2 Hz, 1H), 7.44-7.41 (m, 2H), 7.37-7.35 (m, 2H), 7.29 (t, J = 7.2 Hz, 1H); ^{13}C NMR (DMSO-d_6, 150 MHz) δ 166.9, 163.0, 155.0, 147.3, 136.0, 134.1, 133.7, 130.0, 129.1, 127.2, 126.9, 126.5, 126.3, 126.0, 125.6, 124.3, 121.0, 118.2, 110.0, 81.9; HRMS-ESI(-) *m/z* calcd for $C_{21}H_{15}N_4O_4$ 387.1093 $[M-H]^-$, found 387.1117.

Biology

Reagents

Biologicals. Recombinant HIV-1 reverse transcriptase (RT) was expressed and purified as previously described.[36] P4R5 HIV infection indicator cells were obtained from the NIH AIDS Reagent Program, Division of AIDS, NIAID, NIH (p4R5.MAGI from Dr. Nathaniel Landau). These cells express CD4, CXCR4 and CCR5 as well as a β-galactosidase reporter gene under the control of an HIV LTR promoter.

Chemicals. DNA and RNA oligonucleotides for the preparation of RNA/DNA duplexes for assay of RNase H activity were purchased from Trilink (San Diego, CA).

RNase H assay

RNase H activity was measured essentially as previously described.[31, 37] Full-length HIV RT was incubated with the RNA/DNA duplex substrate HTS-1 (RNA 5'-gaucugagccugggagcu -3'-fluorescein annealed to DNA 3'-CTAGACTCGGACCCTCGA -5'-Dabcyl), a high sensitivity duplex that assesses non-specific internal cleavage of the RNA strand, in the presence of various concentrations of compound. Results were analyzed using "Prism" software (GraphPad Software, San Diego, CA) for nonlinear regression to fit dose-response data to logistic curve models.

RT polymerase assay

RT pol assays were carried out in 96-well plates by measuring the extension of an 18 nucleotide DNA primer (5'-GTCACTGTTCGAGCACA-3') annealed to a 100 nucleotide DNA template (5'-ATGTGTGTGCCCGTCTGTTGTGTGACTCTGGTAACTAGAGATCCCTCAGACCCTTTTAGTCAGTGTGGAATATCTCATAGCTTGGTGCTCGAACAGTGAC-3'). Reactions containing

20 nM RT, 40 nM template/primer, and 10 μM deoxynucleotide triphosphates (dNTPs) in a buffer containing 50 mM Tris (pH 7.8) and 50 mM NaCl were initiated by the addition of 6 mM $MgCl_2$. Reactions contained 1% DMSO and increasing concentrations of compounds. DNA synthesis was carried out for 30 min at 37 °C, and reactions were arrested by the addition of 100 mM EDTA. The QuantiFluor dsDNA System (Promega) was used to quantify the amount of formed double-stranded DNA. Reactions were read at ex/em 504/531 nm in a PerkinElmer EnSpire Multilabel plate reader. Results were analyzed using "Prism" software (GraphPad Software, San Diego, CA) for nonlinear regression to fit dose-response data to logistic curve models.[28]

HIV IN assay

HIV integrase was expressed and purified as previously reported.[38] Inhibition assays were performed using a modified protocol of our reported method.[38] Briefly, 2.1 μL of compound suspended in DMSO was placed in duplicate into a Black 96 well non-binding plate (Corning). Compounds were plated in duplicate to a final concentration of 0.13 — 100 μM. To each well of the plate, 186.9 μL of reaction mixture without DNA substrate was added (10 mM HEPES pH 7.5, 10 % w/v glycerol, 10 mM $MnCl_2$, 1 mM DTT, 1 μM integrase). The enzyme was incubated with inhibitor for 10 min at 25 °C after which the reaction was initiated by the addition of 21 μL of 500 nM oligo (5' biotin ATGTGGAAAATCTCTAGCA annealed with ACTGCTAGAGATTTTCCACAT 3' Cy5). Reactions were incubated at 37 °C for 30 min and then quenched by the addition of 5.2 μL 500 mM EDTA. Each reaction was moved (200 μL) to a MultiScreen HTS PCR plate (Millipore) containing 20 μL streptavidin agarose beads (Life Technologies) and incubated with shaking for 30 min. A vacuum manifold was used to remove

the reaction mixture and the beads were similarly washed 3 times with wash buffer (0.05% SDS, 1 mM EDTA in PBS). The plates were further washed 3 times with 200 µL 50 mM NaOH to denature DNA not covalently linked to the biotin modification. For each denaturation step the plate was incubated with shaking at 25 °C for 5 min and the NaOH was removed by centrifugation at 1000 g for 1 min. The reaction products were eluted from the beads by the addition of 150 µL formamide. The plate was incubated at 25 °C for 10 min and read directly at 635/675 in a SpectraMax i3 plate reader (Molecular Devices).

Antiviral assays

MAGI assays were carried out using P4R5 indicator cells essentially as previously described.[39] P4R5 cells were cultured in 96-well microplates with 4×10^3 cells per well and maintained in DMEM/10% FBS supplemented with puromycin (1 µg/mL). Cells were incubated with either 1% DMSO or varying concentrations of the drugs for 24 h and then exposed to HIV-1 (MOI of 1.25) followed by an additional incubation period of 48 h. The extent of infection was assessed using a fluorescence-based β-galactosidase detection assay, as previously described with minor modifications.[40] After the 48 h incubation period, cells were lysed and 4-methylumbelliferylgalactoside (MUG) substrate was added. The β-galactosidase produced during infection acts on the MUG substrate and yields a fluorescent product, 4-methylumbelliferone (4-MU), that could be detected fluorimetrically with excitation wavelength 365 nm and emission wavelength 446 nm.

Molecular modeling

All modeling experiments were done using the Schrödinger Small Molecule Discovery Suite.[39]

Small Molecules. 2D structures of compounds **8** and **9** were prepared by the LigPrep™ module, which converts 2D structures to 3D, performs energy minimization, and predicts protonated and deprotonated states at physiological pH based on calculated pK_a values for ionizable hydrogens. For compound **8**, pK_a for the hydroxyl attached to nitrogen atom was predicted to be around pH 7.07±1, which indicates that both protonated and deprotonated forms of **8** will likely be present at physiological pH. However, in chelating divalent cations at the active center, the deprotonated form will be more effective due to negative charge and better availability of oxygen lone pairs to overlap with metal orbitals. pK_a of the central hydroxyl on compound **9** was calculated to be pH 4.07±2, indicating that compound **9** is mainly present in its deprotonated form at physiological pH. Thus, deprotonated forms of **8** and **9** were used for docking into the RNase H active site.

Protein Receptors. All studied HIV-1 RT structures were obtained from the Protein Data Bank (PDB). The Protein Preparation Wizard ™ module was used to add hydrogen atoms, minimize energy, and create appropriate protonation states of amino acid side chains. The docking grid was centered on the active site metal cations. Van der Waals radii of non-polar atoms were scaled by 0.8 scaling factor to account for some flexibility of protein backbone and amino acid side chains.

HIV-RT complex with DNA:RNA hybrid (PDB code 1HYS[40]) was used as the main protein structure for docking studies. In structure DNA:RNA hybrid is long enough to reach the RNaseH active center. However, 1HYS structure lacks divalent metal cations in RNaseH active center, which are essential for coordination of active site inhibitor. We manually added two manganese cations to the PDB structure file of 1HYS. The metal coordination geometry solved in the PDB 3IG1[15] structure was used to set distances and angles between active site residues D443, E478, D498, and D549 and metal cations. After manual addition of metal cations, the protein structure

was subjected to energy minimization. A structure without DNA:RNA hybrid was also prepared by manual deletion of the nucleic acid chains from the PDB file.

Docking. Docking simulations were performed with the Glide™ docking algorithm at standard precision. Docking was performed with and without RNA:DNA hybrid present. Coulombic and van der Waals interactions of **8** and **9** with individual amino acid residues were calculated and analyzed. Ligand poses with the most negative docking scores were used for further analysis.

ASSOCIATED CONTENT

Supporting Information Available. Synthesis and characterization data of intermediates **12**–**17**, and molecular formula strings. This material is available free of charge *via* the Internet at http://pubs.acs.org.

AUTHOR INFORMATION

***Corresponding Author**

Email: wangx472@umn.edu; Phone: +1 (612) 626-7025.

 # Present Address

College of Natural and Applied Sciences, University of Guam, Mangilao, Guam 96923, USA.

ACKNOWLEDGMENTS

This research was supported by the National Institutes of Health (AI100890 to SGS, MAP and ZW).

ABBREVIATIONS USED

HIV, human immunodeficiency virus; RT, reverse transcriptase; RNase H, ribonuclease H; HPD, 3-hydroxypyrimidine-2,4-dione; SAR, structure-activity-relationship; HAART, highly active

antiretroviral therapy; IN, integrase; PR, protease; NRTIs, nucleoside RT inhibitors; NNRTIs, nonnucleoside RT inhibitors; INSTI, integrase strand transfer inhibitor; HID, 2-hydroxyisoquinolinedione; THBNH, trihydroxybenzoyl naphthyl hydrazone; RAL, raltegravir; DTG, dolutegravir.

References

1. Yeni, P., Update on HAART in HIV. *J. Hepatol.* **2006,** *44*, S100-103.
2. FDA-approved HIV medicines: https://aidsinfo.nih.gov/understanding-hiv-aids/fact-sheets/21/58/fda-approved-hiv-medicines (February 27, 2017).
3. Martin, A. R.; Siliciano, R. F., Progress Toward HIV Eradication: Case reports, current efforts, and the challenges associated with cure. *Annu. Rev. Med.* **2016,** *67*, 215-228.
4. Kimata, J. T.; Rice, A. P.; Wang, J., Challenges and strategies for the eradication of the HIV reservoir. *Curr. Opin. Immunol.* **2016,** *42*, 65-70.
5. Beilhartz, G. L.; Gotte, M., HIV-1 Ribonuclease H: Structure, catalytic mechanism and inhibitors. *Viruses* **2010,** *2*, 900-926.
6. Sarafianos, S. G.; Marchand, B.; Das, K.; Himmel, D. M.; Parniak, M. A.; Hughes, S. H.; Arnold, E., Structure and function of HIV-1 reverse transcriptase: molecular mechanisms of polymerization and inhibition. *J. Mol. Biol.* **2009,** *385*, 693-713.
7. Cihlar, T.; Ray, A. S., Nucleoside and nucleotide HIV reverse transcriptase inhibitors: 25 years after zidovudine. *Antiviral Res.* **2010,** *85*, 39-58.
8. Singh, K.; Marchand, B.; Kirby, K. A.; Michailidis, E.; Sarafianos, S. G., Structural aspects of drug resistance and inhibition of HIV-1 reverse transcriptase. *Viruses* **2010,** *2*, 606-638.

9. de Bethune, M. P., Non-nucleoside reverse transcriptase inhibitors (NNRTIs), their discovery, development, and use in the treatment of HIV-1 infection: a review of the last 20 years (1989-2009). *Antiviral Res.* **2010,** *85*, 75-90.
10. Parniak, M. A., Unpublishd data,
11. Das, K.; Martinez, S. E.; Bandwar, R. P.; Arnold, E., Structures of HIV-1 RT-RNA/DNA ternary complexes with dATP and nevirapine reveal conformational flexibility of RNA/DNA: insights into requirements for RNase H cleavage. *Nucleic Acids Res.* **2014,** *42*, 8125-8137.
12. Nowotny, M., Retroviral integrase superfamily: the structural perspective. *EMBO Rep.* **2009,** *10*, 144-151.
13. Corona, A.; Masaoka, T.; Tocco, G.; Tramontano, E.; Le Grice, S. F., Active site and allosteric inhibitors of the ribonuclease H activity of HIV reverse transcriptase. *Future Med. Chem.* **2013,** *5*, 2127-2139.
14. Klumpp, K.; Hang, J. Q.; Rajendran, S.; Yang, Y. L.; Derosier, A.; In, P. W. K.; Overton, H.; Parkes, K. E. B.; Cammack, N.; Martin, J. A., Two-metal ion mechanism of RNA cleavage by HIV RNase H and mechanism-based design of selective HIV RNase H inhibitors. *Nucleic Acids Res.* **2003,** *31*, 6852-6859.
15. Billamboz, M.; Bailly, F.; Lion, C.; Touati, N.; Vezin, H.; Calmels, C.; Andreola, M. L.; Christ, F.; Debyser, Z.; Cotelle, P., Magnesium chelating 2-hydroxyisoquinoline-1,3(2H,4H)-diones, as inhibitors of HIV-1 integrase and/or the HIV-1 reverse transcriptase ribonuclease H domain: discovery of a novel selective inhibitor of the ribonuclease H function. *J. Med. Chem.* **2011,** *54*, 1812-1824.

16. Billamboz, M.; Suchaud, V.; Bailly, F.; Lion, C.; Demeulemeester, J.; Calmels, C.; Andreola, M. L.; Christ, F.; Debyser, Z.; Cotelle, P., 4-Substituted 2-hydroxyisoquinoline-1,3(2H,4H)-diones as a novel class of HIV-1 integrase inhibitors. *ACS Med. Chem. Lett.* **2013,** *4*, 41-46.
17. Himmel, D. M.; Maegley, K. A.; Pauly, T. A.; Bauman, J. D.; Das, K.; Dharia, C.; Clark, A. D., Jr.; Ryan, K.; Hickey, M. J.; Love, R. A.; Hughes, S. H.; Bergqvist, S.; Arnold, E., Structure of HIV-1 reverse transcriptase with the inhibitor beta-thujaplicinol bound at the RNase H active site. *Structure* **2009,** *17*, 1625-1635.
18. Himmel, D. M.; Myshakina, N. S.; Ilina, T.; Van Ry, A.; Ho, W. C.; Parniak, M. A.; Arnold, E., Structure of a dihydroxycoumarin active-site inhibitor in complex with the RNase H domain of HIV-1 reverse transcriptase and structure-activity analysis of inhibitor analogs. *J. Mol. Biol.* **2014,** *426*, 2617-2631.
19. Shaw-Reid, C. A.; Munshi, V.; Graham, P.; Wolfe, A.; Witmer, M.; Danzeisen, R.; Olsen, D. B.; Carroll, S. S.; Embrey, M.; Wai, J. S.; Miller, M. D.; Cole, J. L.; Hazuda, D. J., Inhibition of HIV-1 ribonuclease H by a novel diketo acid, 4-[5-(benzoylamino)thien-2-yl]-2,4-dioxobutanoic acid. *J. Biol. Chem.* **2003,** *278*, 2777-2780.
20. Lansdon, E. B.; Liu, Q.; Leavitt, S. A.; Balakrishnan, M.; Perry, J. K.; Lancaster-Moyer, C.; Kutty, N.; Liu, X.; Squires, N. H.; Watkins, W. J.; Kirschberg, T. A., Structural and binding analysis of pyrimidinol carboxylic acid and N-hydroxy quinazolinedione HIV-1 RNase H inhibitors. *Antimicrob. Agents Chemother.* **2011,** *55*, 2905-2915.
21. Williams, P. D.; Staas, D. D.; Venkatraman, S.; Loughran, H. M.; Ruzek, R. D.; Booth, T. M.; Lyle, T. A.; Wai, J. S.; Vacca, J. P.; Feuston, B. P.; Ecto, L. T.; Flynn, J. A.; DiStefano, D. J.; Hazuda, D. J.; Bahnck, C. M.; Himmelberger, A. L.; Dornadula, G.; Hrin, R. C.; Stillmock, K. A.; Witmer, M. V.; Miller, M. D.; Grobler, J. A., Potent and selective HIV-1 ribonuclease H

inhibitors based on a 1-hydroxy-1,8-naphthyridin-2(1H)-one scaffold. *Bioorg. Med. Chem. Lett.* **2010,** *20*, 6754-6757.

22. Beilhartz, G. L.; Ngure, M.; Johns, B. A.; Deanda, F.; Gerondelis, P.; Gotte, M., Inhibition of the ribonuclease H activity of HIV-1 reverse transcriptase by GSK5750 correlates with slow enzyme-inhibitor dissociation. *J. Biol. Chem.* **2014**, 16270-16277.
23. Wu, B.; Tang, J.; Wilson, D. J.; Huber, A. D.; Casey, M. C.; Ji, J.; Kankanala, J.; Xie, J.; Sarafianos, S. G.; Wang, Z., 3-Hydroxypyrimidine-2,4-dione-5-N-benzylcarboxamides potently inhibit HIV-1 integrase and RNase H. *J. Med. Chem.* **2016,** *59*, 6136-6148.
24. Kankanala, J.; Kirby, K. A.; Liu, F.; Miller, L.; Nagy, E.; Wilson, D. J.; Parniak, M. A.; Sarafianos, S. G.; Wang, Z. Q., Design, synthesis, and biological evaluations of hydroxypyridonecarboxylic acids as inhibitors of HIV reverse transcriptase associated RNase H. *J. Med. Chem.* **2016,** *59*, 5051-5062.
25. Tang, J.; Liu, F.; Nagy, E.; Miller, L.; Kirby, K. A.; Wilson, D. J.; Wu, B. L.; Sarafianos, S. G.; Parniak, M. A.; Wang, Z., 3-Hydroxypyrimidine-2,4-diones as selective active site inhibitors of HIV reverse transcriptase-associated RNase H: design, synthesis, and biochemical evaluations. *J. Med. Chem.* **2016,** *59*, 2648-2659.
26. Vernekar, S. K. V.; Liu, Z.; Nagy, E.; Miller, L.; Kirby, K. A.; Wilson, D. J.; Kankanala, J.; Sarafianos, S. G.; Parniak, M. A.; Wang, Z. Q., Design, synthesis, biochemical, and antiviral evaluations of C6 benzyl and C6 biarylmethyl substituted 2-hydroxylisoquinoline-1,3-diones: dual Inhibition against HIV reverse transcriptase-associated RNase H and polymerase with antiviral activities. *J. Med. Chem.* **2015,** *58*, 651-664.

27. Wu, B. L.; Tang, J.; Wilson, D. J.; Huber, A. D.; Casey, M. C.; Ji, J.; Kankanala, J.; Xie, J. S.; Sarafianos, S. G.; Wang, Z. Q., 3-Hydroxypyrimidine-2,4-dione-5-N-benzylcarboxamides potently inhibit HIV-1 integrase and RNase H. *J. Med. Chem.* **2016,** *59*, 6136-6148.

28. Tang, J.; Kirby, K. A.; Huber, A. D.; Casey, M. C.; Ji, J.; Wilson, D. J.; Sarafianos, S. G.; Wang, Z., 6-Cyclohexylmethyl-3-hydroxypyrimidine-2,4-dione as an inhibitor scaffold of HIV reverase transcriptase: impacts of the 3-OH on inhibiting RNase H and polymerase. *Eur. J. Med. Chem.* **2017,** *128*, 168-179.

29. Tang, J.; Maddali, K.; Dreis, C. D.; Sham, Y. Y.; Vince, R.; Pommier, Y.; Wang, Z. Q., N-3 Hydroxylation of pyrimidine-2,4-diones yields dual inhibitors of HIV reverse transcriptase and integrase. *ACS Med. Chem. Lett.* **2011,** *2*, 63-67.

30. Tang, J.; Maddali, K.; Metifiot, M.; Sham, Y. Y.; Vince, R.; Pommier, Y.; Wang, Z. Q., 3-Hydroxypyrimidine-2,4-diones as an inhibitor scaffold of HIV integrase. *J. Med. Chem.* **2011,** *54*, 2282-2292.

31. Vernekar, S. K.; Liu, Z.; Nagy, E.; Miller, L.; Kirby, K. A.; Wilson, D. J.; Kankanala, J.; Sarafianos, S. G.; Parniak, M. A.; Wang, Z., Design, synthesis, biochemical, and antiviral evaluations of C6 benzyl and C6 biarylmethyl substituted 2-hydroxylisoquinoline-1,3-diones: dual inhibition against HIV reverse transcriptase-associated RNase H and polymerase with antiviral activities. *J. Med. Chem.* **2015,** *58*, 651-664.

32. Sirivolu, V. R.; Vernekar, S. K. V.; Ilina, T.; Myshakina, N. S.; Parniak, M. A.; Wang, Z. Q., Clicking 3 '-azidothymidine into novel potent inhibitors of human immunodeficiency virus. *J. Med. Chem.* **2013,** *56*, 8765-8780.

33. Himmel, D. M.; Sarafianos, S. G.; Dharmasena, S.; Hossain, M. M.; McCoy-Simandle, K.; Ilina, T.; Clark, A. D.; Knight, J. L.; Julias, J. G.; Clark, P. K.; Krogh-Jespersen, K.; Levy, R. M.;

Hughes, S. H.; Parniak, M. A.; Arnold, E., HIV-1 reverse transcriptase structure with RNase H inhibitor dihydroxy benzoyl naphthyl hydrazone bound at a novel site. *ACS Chem. Biol.* **2006,** *1*, 702-712.

34. Summa, V.; Petrocchi, A.; Bonelli, F.; Crescenzi, B.; Donghi, M.; Ferrara, M.; Fiore, F.; Gardelli, C.; Gonzalez Paz, O.; Hazuda, D. J.; Jones, P.; Kinzel, O.; Laufer, R.; Monteagudo, E.; Muraglia, E.; Nizi, E.; Orvieto, F.; Pace, P.; Pescatore, G.; Scarpelli, R.; Stillmock, K.; Witmer, M. V.; Rowley, M., Discovery of raltegravir, a potent, selective orally bioavailable HIV-integrase inhibitor for the treatment of HIV-AIDS infection. *J. Med. Chem.* **2008,** *51*, 5843-5855.
35. Johns, B. A.; Kawasuji, T.; Weatherhead, J. G.; Taishi, T.; Temelkoff, D. P.; Yoshida, H.; Akiyama, T.; Taoda, Y.; Murai, H.; Kiyama, R.; Fuji, M.; Tanimoto, N.; Jeffrey, J.; Foster, S. A.; Yoshinaga, T.; Seki, T.; Kobayashi, M.; Sato, A.; Johnson, M. N.; Garvey, E. P.; Fujiwara, T., Carbamoyl pyridone HIV-1 integrase inhibitors 3. A diastereomeric approach to chiral nonracemic tricyclic ring systems and the discovery of dolutegravir (S/GSK1349572) and (S/GSK1265744). *J. Med. Chem.* **2013,** *56*, 5901-5916.
36. Fletcher, R. S.; Holleschak, G.; Nagy, E.; Arion, D.; Borkow, G.; Gu, Z.; Wainberg, M. A.; Parniak, M. A., Single-step purification of recombinant wild-type and mutant HIV-1 reverse transcriptase. *Protein Expres. Purif.* **1996,** *7*, 27-32.
37. Parniak, M. A.; Min, K. L.; Budihas, S. R.; Le Grice, S. F.; Beutler, J. A., A fluorescence-based high-throughput screening assay for inhibitors of human immunodeficiency virus-1 reverse transcriptase-associated ribonuclease H activity. *Anal. Biochem.* **2003,** *322*, 33-39.
38. Wang, Z.; Bennett, E. M.; Wilson, D. J.; Salomon, C.; Vince, R., Rationally designed dual inhibitors of HIV reverse transcriptase and integrase. *J. Med. Chem.* **2007,** *50*, 3416-3419.

39. Sirivolu, V. R.; Vernekar, S. K. V.; Ilina, T.; Myshakina, N. S.; Parniak, M. A.; Wang, Z., Clicking 3 '-azidothymidine into novel potent inhibitors of human immunodeficiency virus. *J. Med. Chem.* **2013,** *56*, 8765-8780.

40. Abram, M. E.; Parniak, M. A., Virion instability of human immunodeficiency virus type 1 reverse transcriptase (RT) mutated in the protease cleavage site between RT p51 and the RT RNase H domain. *J. Virol.* **2005,** *79*, 11952-11961.

TOC Graphic

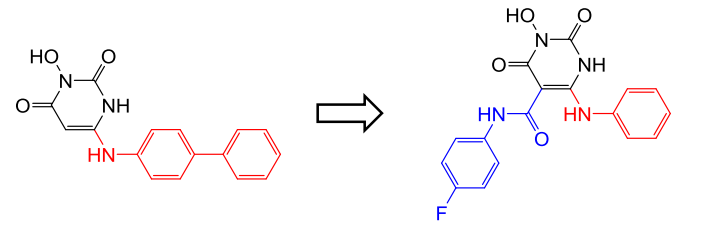

RNase H IC_{50} = 0.25 μM
HIV-1 EC_{50} >25μM

Single-winged HPD

RNase H IC_{50} = 0.004 μM
HIV-1 EC_{50} = 6.1 μM

Double-winged HPD